Human vision sequentially prioritizes expected and unexpected information

AUTHORs: *Arjen ALINK[12], Janika BECKER[1], Helen BLANK[134];

[1]Dept. of Systems Neurosci., University Medical Center Hamburg-Eppendorf, Hamburg, Germany

[2]Institute of Medical Psychology, Center of Brain, Behavior and Metabolism (CBBM), University of Lübeck, Lübeck, Germany

[3]Faculty of Psychology, Ruhr University Bochum, Bochum, Germany,

[4]Research Center One Health Ruhr, University Alliance Ruhr, Bochum, Germany

Summary

This electroencephalography (EEG) study reveals how expectations dynamically shape visually evoked brain responses through a biphasic temporal mechanism: an early enhancement of encoding for expected image components, followed by a later prioritization of unexpected components. This temporal dissociation suggests that the brain initially integrates sensory input with prior expectations in a Bayesian manner before shifting to emphasize surprising information, thereby supporting both efficient recognition and adaptive model updating. Notably, this updating process first amplifies category-level representations before increasing the encoding of image identity.

Introduction

Several decades ago, a paper by Rao and Ballard[1] reinvigorated the Helmholtzian idea that perception arises from a synergy between sensations and expectations. Since then, a large cohort of human neuroimaging studies[3,5,7] has interpreted contextual effects on brain activity in sensory cortices within the theoretical framework of predictive coding (PC framework), which emphasises the importance of prediction-error coding, enhanced neural representations of unexpected stimuli.

The resulting empirical landscape, however, remains difficult to reconcile into a coherent account of how expectations shape sensory processing. Most notably, conflicting evidence suggests that expectations can lead to either enhanced or reduced fidelity of sensory representations of expected stimuli, processes referred to as 'sharpening' and 'dampening,' respectively[5,7,9,11]. This divergence leaves open a fundamental question: does expectation exert a 'prediction-error' effect by suppressing redundant information, or a 'Bayesian' effect by selectively enhancing the precision of expected signals?

To address this open question, we conducted an EEG experiment designed to compare the relative neural encoding strength of expected and unexpected image components over time. Specifically, we tested whether expectation facilitates an initial Bayesian effect followed by a subsequent prediction-error signaling phase, consistent with the dual-process theory proposed by Press and colleagues[13]. To this end, we measured how expectation influences the extent to which EEG signals encode the identity and category (animacy) of image components over time. This approach also clarifies whether expectation effects arise during early sensory processing or are more characteristic of later, higher-order cognitive stages, and whether expectation differentially affects image-specific representations versus more abstract category-level representations.

Results

During our EEG study, participants viewed four natural images depicting a car, a house, a cat, and an elephant. During each 1.5-hour EEG session, these images were presented in a fixed repeating order (e.g., car–house–cat–elephant–car–house–cat–elephant…, as shown in Fig. 1a). Participants viewed this sequence more than 2,500 times per session, rendering the occurrence of each image highly predictable. Each participant completed six EEG sessions, across which they were shown all six possible unique image sequences. Data analysis was performed across all six sessions for each participant to rule out low-level perceptual sequence effects, including adaptation-related transition-patterns[15]. Participants were instructed to continuously fixate the central fixation cross and, to ensure that they remained vigilant and attended to all images, we asked them to press a button whenever an upside-down image was presented. These catch trials were shown during 1.6% of all trials, and participants detected them during 97.1% (SD = 2.8%) of all trials with an average reaction time of 663 ms (SD = 79 ms).

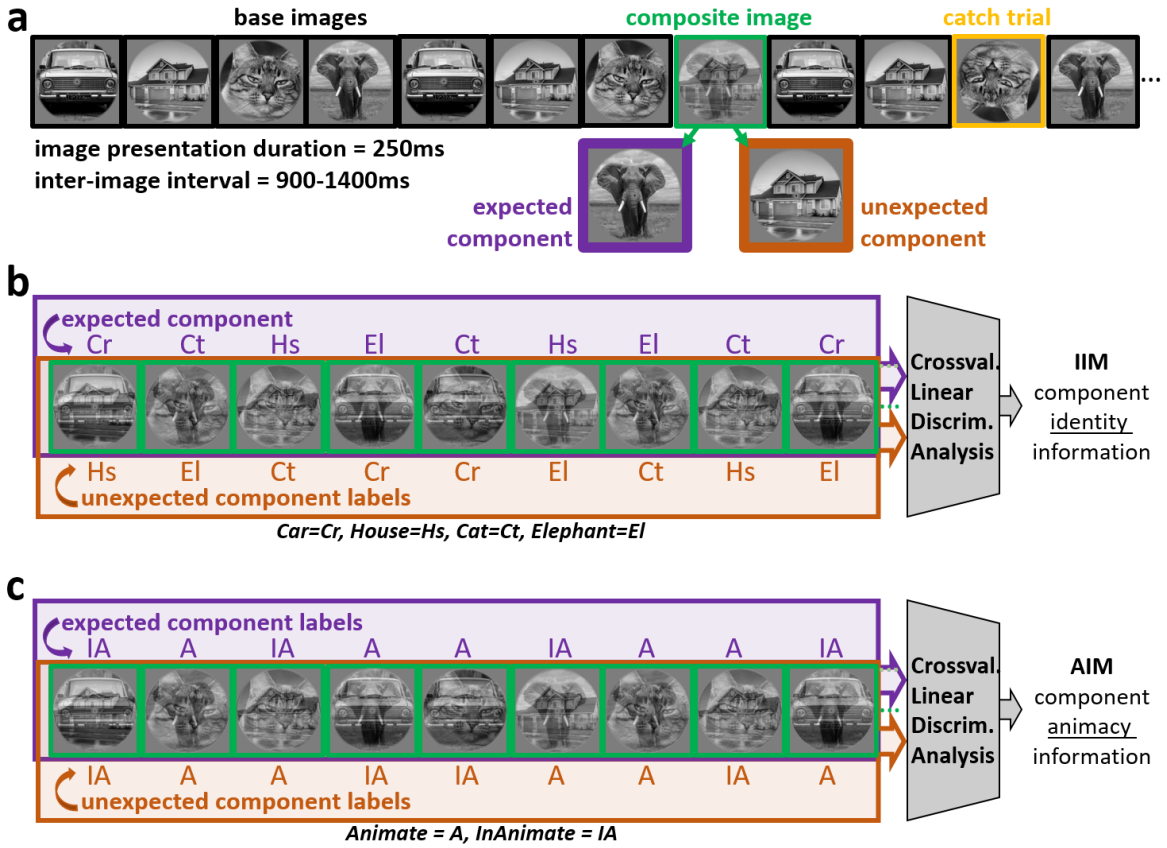

Figure 1 | Experimental design and data analysis

a) EEG experimental paradigm. *Participants viewed a continuous, highly predictable stream of four base images presented in a fixed repeating order (e.g., car→house→cat→elephant...). Each image was presented for 250 ms, separated by a variable inter-image interval of 900–1400 ms. In 24% of trials, a composite image (green outline) was presented, formed by superimposing the predicted image (expected component; purple outline) and a surprising image (unexpected component; brown outline). Participants maintained vigilance by detecting infrequent (1.6%) catch trials depicting upside-down images (yellow outline).* ***b) Image Identity Measure (IIM)*** *To measure neural encoding of image identity during composite image presentations, cross-validated Linear Discriminant Analysis (LDA) was applied to EEG data. Classifiers were trained and tested separately using labels corresponding to the identity of the expected component (purple upper box) or the identity of the unexpected component (brown lower box).* ***c) Animacy Information Measure (AIM)*** *Analogous to the IIM analysis, LDA was used to quantify animacy encoding. Composite images were labeled according to whether their expected components (purple upper box) or unexpected components (brown lower box) were animate.*

Critically, during 24% of image presentations, we showed a composite image consisting of the expected image and an unexpected image (Figure 1a). These composite images allowed us to examine image-identity encoding separately for the expected and unexpected components by labeling each composite according to either the identity of its expected or unexpected component (Figure 1b). Moreover, to examine animacy encoding, we also labeled the composite images according to whether their expected and unexpected components were animate or inanimate (Fig 1c). To measure these two types of image component information encoding, we applied Linear Discriminant Analysis (LDA) separately for each electrode and labeling scheme to quantify each component's identity information (IIM) and animacy information (AIM) over time. These two measures were computed based on the cross-validated posterior probability values of image components, as described in more detail in the Star★Methods Section.

As a sanity check, we first quantified IIMs and AIMs for the base images. Consistent with previous work[16,17], this analysis revealed robust decodability of base-image identity and animacy from 68 ms and 136 ms after stimulus onset, respectively (Supplemental Figure). Identity and animacy were also decodable for both expected and unexpected components at levels clearly above chance (Fig. 2 a,b,d,e), although overall less strongly than in the base trials. This reduction was anticipated, given that for the composite images, the LDA classifier had to extract information from lower-contrast images while simultaneously unmixing them from the overlapping component images.

For the expected image components (Fig. 2a), identity information rose significantly above chance from 104 ms onward, with the strongest effects over occipital, parietal, and temporal electrodes (all corr. $P < 0.005$; $t(14399) = 3.24–14.70$; IIM = 0.0003–0.0041). For the unexpected components (Fig. 2b), identity information exceeded chance from 116 ms, showing a broadly similar topography but with additional significant effects over frontal electrodes (all corr. $P < 0.005$; $t(14399) = 3.19–13.73$; IIM = 0.0003–0.0037). A direct comparison of IIM values for expected versus unexpected components (Fig. 2c) revealed two clusters of expectation-related differences. The earlier cluster (304–328 ms) showed enhanced encoding of expected component identity across a right parieto-occipital electrode cluster (all corr. $P < 0.005$; $t(14399) = -4.02$ to -6.93; IIM difference = -0.0006 to -0.0024). In contrast, the later cluster (460–472 ms) showed enhanced encoding of unexpected component identity across a left parieto-occipital cluster (all corr. $P < 0.005$; $t(14399) = 3.96$ to 5.55; IIM difference = 0.0007 to 0.0013). Together, these findings indicate that expectation initially boosts identity encoding for expected components, followed by enhanced encoding of unexpected component identity at later stages. Having established these

expectation-related differences in identity processing, we next examined whether a similar temporal pattern would emerge for animacy information.

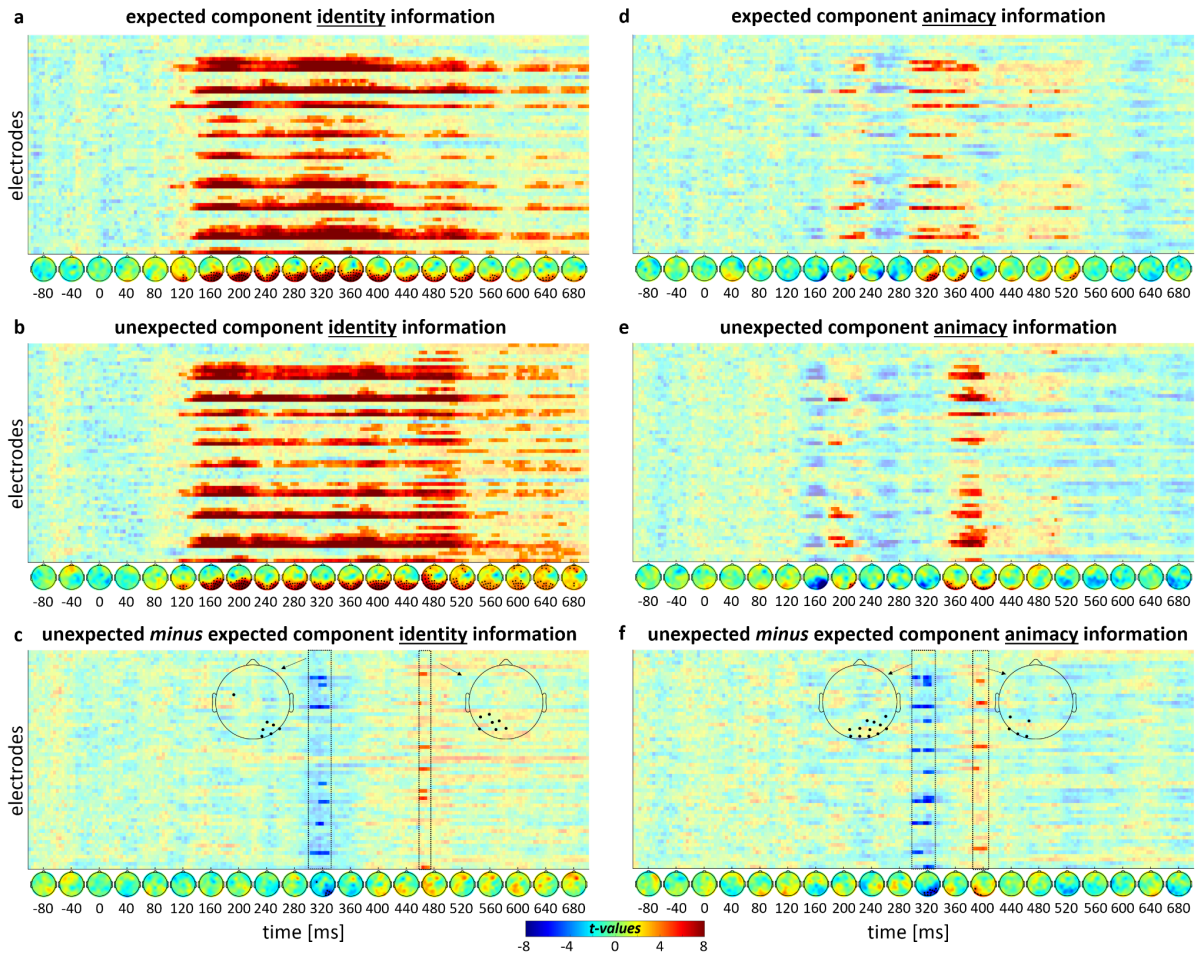

Figure 2 | component identity and animacy information and their modulation by expectation

*Each matrix displays t-values, with rows representing individual electrodes and columns representing timepoints. Non-significant t-values are faded. Below each matrix, the same t-values are shown as topographic plots for selected timepoints from −80 to 680 ms in 40-ms steps. Significant electrode locations in these topographic plots are marked with a black dot. Matrices **a** and **b** show t-statistics based on comparing observed image identity measures (IIMs) to chance level for the expected and unexpected components, respectively. Matrices **d** and **e** show t-statistics based on comparing observed image animacy measures (AIMs) to zero for the expected and unexpected components, respectively. Matrices **c** and **f** display t-statistics for IIM and AIM difference values (unexpected minus expected). Superimposed on matrices c and f are empty topographic plots indicating the locations of all significant electrodes for each cluster of effects, corresponding to the adjacent dotted boxes superimposed on the matrices. The electrode labels for these clusters are: (c) positive IIM effects: P4,*

O2, P8, FC3, PO4, P6, PO8, negative IIM effects: P3, P7, CP5, P1, CP3, PO3, POz, (f) positive AIM effects: P4, O1, O2, P8, Oz, CP6, P2, PO3, PO4, P6, PO8, POz, negative AIM effects: O1, P7, CP5, P1, PO7. T-tests for AIM and IIM values versus chance (a, b, d, e) were one-sided (positive direction). T-tests for the difference measures (c, f) were two-sided. All highlighted significant effects survived FDR correction at p < .005.

For expected components (Fig. 2d), animacy information rose significantly above chance from 196 ms onward, with the strongest effects over right-lateralized occipital, parietal, and temporal electrodes (all corr. P < 0.005; t(14399) = 3.65–7.98; AIM = 0.0008–0.0033). For unexpected components (Fig. 2e), animacy information exceeded chance from 180 ms, with the strongest effects over left-lateralized occipital, parietal, temporal, and frontal electrodes (all corr. P < 0.005; t(14399) = 3.58 to 8.42; AIM = 0.0006–0.0033). A direct comparison of AIM values (Fig. 2f) revealed two clusters of expectation-related differences. The earlier cluster (300–328 ms) showed enhanced encoding of expected component animacy across a parieto-occipital cluster (all corr. P < 0.005; t(14399) = -3.96 to -6.76; AIM difference = -0.0013 to -0.0035). The later cluster (388–404 ms), in contrast, showed enhanced encoding of unexpected component animacy across a left parieto-occipital cluster (all corr. P < 0.005; t(14399) = 4.02 to 5.98; AIM difference = 0.0012 to 0.0025).

Discussion

Taken together, the identity and animacy results reveal a consistent temporal pattern of how expectations shape visual encoding. For both features, expectation initially enhances the encoding of the expected image components, suggesting an early phase during which prior knowledge is integrated with sensory input to support veridical perception. This early facilitation was followed by a later phase during which encoding was stronger for the unexpected components, indicating increased processing of surprising information. This biphasic pattern, therefore, provides direct support for the proposal that perceptual expectations first promote Bayesian integration to optimize current perceptual inferences, and subsequently amplify the encoding of unexpected events to refine future predictions[13].

When comparing the temporal dynamics of expectation effects on animacy and identity encoding, a striking difference becomes apparent. Although expectation enhances the encoding of expected component identity and animacy within the same temporal window, the subsequent enhancement for unexpected components unfolds differently across the two feature domains. Specifically, animacy

encoding for unexpected components is boosted by expectation 72 ms earlier than identity encoding. This temporal offset suggests that surprising stimuli first trigger an increased awareness of the kind of unexpected event that occurred, its broad, categorical "gist", before the system resolves the more fine-grained perceptual details needed to identify what exactly was surprising. In this sense, our findings resonate with the broader "forest before the trees" principle articulated in reverse hierarchy theory[18], in which coarse, global representations are accessed earlier and guide the subsequent refinement of detailed perceptual interpretations.

All expectation-related effects we observed emerged no earlier than 300 ms after stimulus onset, far too late to reflect modulation of the initial feedforward sweep. This timing is later than recently reported expectation effects on EEG responses[19], but it aligns with studies that suggest that expectation effects are predominantly cognitive rather than strictly perceptual in nature[20,21] . The temporal profile of our effects also overlaps with the highly discussed N400 component[22]. Although interpretations of the N400 vary, from semantic retrieval and contextual integration to signaling prediction error, contemporary accounts increasingly view it as a graded index of contextual facilitation and prediction-confirmation during semantic access[23]. The succession of opposing expectation effects we observe refines and unifies these perspectives: expectations modulate brain activity through a biphasic mechanism, with an initial enhancement of encoding for expected image components followed by a later prioritization of unexpected components. This temporal pattern suggests a dynamic interplay between early facilitation driven by prior knowledge and subsequent prediction-error computations at higher categorical levels, consistent with Bayesian accounts of perception and enabled by recurrent interactions within the visual hierarchy[24]. Our findings also coincide temporally with recurrent high-level effects in the lateral occipital cortex, indicating that prior-induced top-down processing can enhance representations of expected stimulus features[25].

In conclusion, this EEG study reveals that expectations shape visual processing through a biphasic mechanism: the brain first uses prior knowledge to enhance the encoding of expected information, and then shifts to amplify surprising events. Therefore, our data suggests that Bayesian integration of sensory information and enhanced processing of surprising events unfold sequentially rather than simultaneously in the human brain. Intriguingly, for unexpected stimuli, the brain prioritizes the encoding of high-level categorical features before resolving their detailed identity, a pattern that echoes the principles of reverse-hierarchy theory, in which coarse, global representations precede fine-grained perceptual detail. Finally, the relatively late timing of both effects supports recent proposals that expectation effects are more 'cognitive' than 'perceptual' in nature[20].

Resource availability

Lead Contact

Further information and requests for resources should be directed to and will be fulfilled by the lead contact, Arjen Alink, a.alink@uke.de

Materials Availability

This study did not generate new unique reagents.

Data and Code Availability

- Raw EEG data, MATLAB preprocessing, analysis and plotting scripts, stimulus files, and the Python script used for stimulus presentation have been deposited at the Open Science Framework (OSF) and are publicly available as of the date of publication. The DOI/link is listed in the Key Resources Table.
- Any additional information required to reanalyze the data reported in this paper is available from the lead contact upon request.

Acknowledgments

We thank Antoniya Boyanova, Ivana Tanasic and Nahid Hasan for constructive feedback regarding the manuscript. We acknowledge support by the European Research Council (ERC2021-CoG-101044616 to Arjen Alink). This work is funded by the Emmy Noether program of the Deutsche Forschungsgemeinschaft (German Research Foundation; Grant No DFG BL 1736/1-1 to HB).

Author contributions

Conceptualization, A.A. and H.B.; methodology, A.A.; investigation, A.A., J.B., and H.B.; visualization, A.A.; funding acquisition, A.A and H.B.; project administration, A.A. and H.B.; supervision, A.A and H.B.; writing, A.A and H.B.;

Declaration of interests

The authors declare no competing interests.

Declaration of generative AI and AI-assisted technologies in the writing process

During the preparation of this work the authors used ChatGPT-4.0 in order to improve style and readability. After using this tool/service, the authors reviewed and edited the content as needed and take full responsibility for the content of the published article.

STAR★Methods

Key resources table

Reagent or Resource	**Source**	**Identifier**
Deposited Data		
Raw EEG data, stimulus files, and analysis scripts	This paper; OSF	Made available upon publication
Software and Algorithms		
MATLAB Release R2021b	The MathWorks, Inc.	RRID: SCR_001622
EEGLAB toolbox	Delorme & Makeig (2004)	RRID: SCR_007292
PsychoPy	Peirce et al. (2019)	RRID: SCR_006571
SHINE toolbox for MATLAB	Willenbockel et al. (2010)	https://github.com/mwillenbockel/SHINE

BrainVision Recorder	Brain Products	N/A
Other		
64-channel ActiCap	Brain Products, Gilching, Germany	N/A
23-inch TFT-Screen (SyncMaster P2370)	Samsung, Seoul, South Korea	N/A

Experimental model and study participant details

Human Subjects

Six participants took part in six EEG sessions (three females and three males, age range 19 to 38 years). All three authors participated in this study. Experimental procedures were approved by the Ethics Committee of the Chamber of Physicians in Hamburg, and participants provided written informed consent.

Method details

Stimulus Generation and Presentation

Stimuli consisted of four grey-scale natural images of a cat, an elephant, a car, and a house. Images were downloaded from the Pixabay and Unsplash stock photo websites under their free-to-use licences. Images were transformed into grey-scale images, and we applied a fade-out mask to them to make the images' peripheral and central areas grey. Subsequently, we reduced low-level differences across images by applying the spectrum, histogram, and intensity normalisation and equalisation (SHINE) toolbox[2] for MATLAB. All images were presented using PsychoPy on a 23-inch TFT-Screen (SyncMaster P2370; Samsung, Seoul, South Korea) positioned centrally 110 cm in front of

the participant. The circular stimulus area had a radius of 7.24-degree visual angle (°), the central grey area had a radius of .59°, and the black fixation dot had a radius of .08°. Composite images were created while running PsychoPy by drawing one image in the background and drawing the second image with 50% opacity on top of it. All base images were presented with 75% opacity.

We presented these stimuli to participants in a deterministic fixed repeating sequence (as shown in Fig. 1) during six 1.5-hour EEG sessions on six different days. Each of these sessions was subdivided into five ten-minute runs to accommodate short breaks for our participants. We presented each of the six possible repeating sequence orders (1234, 1243, 1324, 1342, 1423, and 1432) once to each participant (n = 6) during one of the six EEG sessions. Note that one can present a fixed repeating sequence of four images in six and not in twenty-four manners because, e.g., the image orders 1234, 2341, 3412, and 4123 give rise to the same repetitive sequence (...1234123412341234…). As a result, each of the four base images and each image component had a perfectly balanced stimulus history across all six sessions. The first image within a sequence was pseudorandomly selected such that each of the four images was shown at least once, but no more than twice, as the first image of a sequence across the six sessions. During a trial, an image was presented for 250 ms followed by a 900-1400 ms inter-stimulus interval, during which only the grey background and the black fixation dot were presented. Participants were instructed to fixate the central fixation dot throughout the experiment and to press a button whenever a catch trial (upside-down base image) was presented.

Note that twelve unique composite images entail the six possible image pairs presented under two different expectation conditions. Hence, the composite image containing the elephant and the house, shown in Figure 1, was presented when a house was expected and when the elephant was expected. Composite images were pseudo-randomly interspersed in the image sequences while ensuring that each composite image was preceded by at least two base images. To preclude the effects of direct repetition, neither the expected nor the unexpected component of each composite image was based on the preceding base image. As a result, across all six sessions, physically identical composite images had the same balanced one-back history across expectation conditions. E.g., cat-house composites were equally often preceded by a car and an elephant stimulus, both for composite images presented when a cat and when a house image was expected.

EEG Recording and Preprocessing

EEG data were sampled at 250 Hz using 64 active electrodes positioned according to the extended 10–20 system (ActiCap, Brain Products, Gilching, Germany) and recorded with BrainVision Recorder.

Preprocessing was performed in MATLAB (The MathWorks, Inc. MATLAB Release R2021b. Natick, Massachusetts, USA (2021), using the EEGLAB toolbox[4], and included standard high- and low-pass filtering at 0.1 Hz and 100 Hz, respectively. The continuous data were then epoched (-200 to 800 ms) and baseline-corrected using the average signal from −200 ms to stimulus onset. No additional preprocessing or artifact-rejection procedures were applied, as such steps are more likely to reduce than enhance statistical power[6].

Quantification and statistical analysis

Because expectation effects in EEG can be subtle and difficult to detect[8], we collected a large amount of data per participant: 2,400 composite-image trials and 10,200 base-image trials for each of our six participants. Data were analysed using a fixed-effects approach, providing high statistical power while acknowledging that the resulting effects cannot be expected to generalize beyond the measured sample.

We performed the LDA analysis separately for each participant, using 10-fold cross-validation, to obtain posterior probability values for left-out base images and for left-out expected and unexpected components of the composite images. Posterior probabilities for composite images were computed after labeling them as either their expected or unexpected components (Fig. 1), yielding image identity measures (IIMs). Analogously, labeling composite images by the animacy of their expected and unexpected components (cat, elephant vs. house, car) yielded raw animacy identity measures (AIM_raw). To obtain AIM values that more specifically reflect animacy rather than idiosyncratic low-level image features, we also computed AIM_control values based on the two alternative pairings (cat, house vs. elephant, car; cat, car vs. elephant, house). These AIM_control values contain no animacy information but capture low-level visual structure we aimed to control for. Final AIM values were therefore computed by subtracting the average AIM_control value from AIM_raw. All IIM and AIM values were computed in a mass-univariate manner, separately for each timepoint and each electrode (excluding eye electrodes, n = 60).

During six of our eight analyses (Figure 2a,b,d,e; Supplemental Figure a,b), we performed one-sided t-tests (positive only) to determine if observed IIM and AIM values were significantly greater than chance level and zero respectively. For base images, this test was applied across all single-image IIMs from all participants. For the expected and unexpected components of the composite images, two separate t-tests were applied across all expected and unexpected component IIMs from all participants. The remaining two analyses (Figure 2c,f) examined how expectation modulated IIM and

AIM values by applying two-sided t-tests, versus zero, to IIM- and AIM-difference values (unexpected minus expected).

To correct for multiple comparisons across electrodes and timepoints, we applied the Benjamini–Hochberg procedure to control the false discovery rate (FDR)[10]. Corrected p-values were thresholded at $p < .005$. To further ensure that the observed effects represented robust neurophysiological signals rather than transient artifacts or spurious statistical noise, we imposed additional spatiotemporal cluster thresholds. First, we discarded significant effects lasting only two consecutive timepoints or fewer (≤ 8ms). This temporal constraint is based on the principle that meaningful ERP components typically span longer durations (e.g., >10–20 ms) due to the underlying kinetics of neural populations[12]. Second, we applied a spatial electrode-cluster threshold, rejecting effects that, at any given timepoint, were supported by fewer than three electrodes. This approach aligns with established cluster-based permutation logic[14], which leverages the fact that neural sources are projected via volume conduction across multiple scalp sensors. By requiring spatial and temporal contiguity, we prioritize effects with high biological plausibility and replicability, effectively filtering out isolated, non-physiologically grounded Type I errors.

Supplemental information

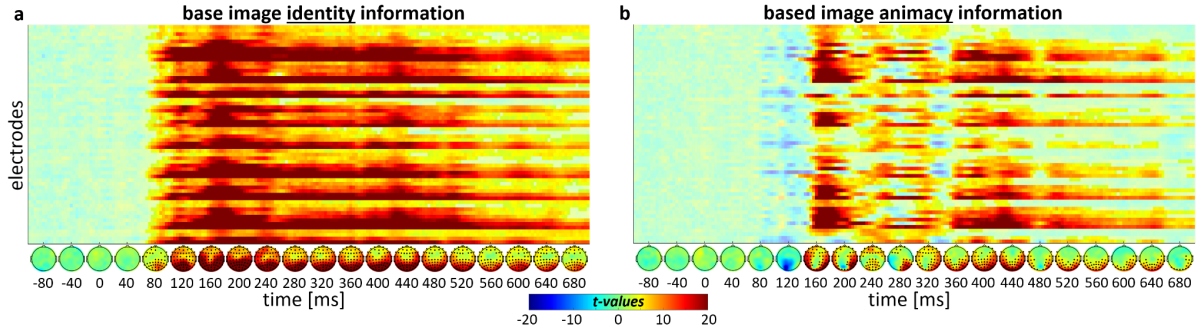

Supplemental Figure | base image identity and animacy information

*Each matrix displays t-values, with rows representing individual electrodes and columns representing timepoints. Non-significant t-values are faded. Below each matrix, the same t-values are shown as topographic plots for selected timepoints from −80 to 680 ms in 40-ms steps. Significant electrode locations in these topographic plots are marked with a black dot. Matrix **a** shows t-statistics based on comparing observed base image identity measures (IIMs) to chance. Matrix **b** shows t-statistics based on comparing observed base image animacy measures (AIMs) versus zero. The t-tests were one-sided (positive direction). All highlighted significant effects survived FDR correction at $p < .005$. Identity and animacy information rose significantly above chance from 68 ms and 136 ms onward respectively (all corr. $P < 0.005$ for identity information: $t(61197) = 2.90$ to 84.54; IIM values minus chance level = 0.0001 to 0.0311, all corr. $P < 0.005$ for animacy information: $t(61197) = 3.04$ to 68.99; AIM values = 0.0001 to 0.0399).*

References

1. Rao, R.P., and Ballard, D.H. (1999). Predictive coding in the visual cortex: a functional interpretation of some extra-classical receptive-field effects. Nat. Neurosci. *2*, 79–87.

2. Willenbockel, V., Sadr, J., Fiset, D., Horne, G.O., Gosselin, F., and Tanaka, J.W. (2010). Controlling low-level image properties: The SHINE toolbox. Behav. Res. Methods *42*, 671–684. https://doi.org/10.3758/BRM.42.3.671.

3. Alink, A., Schwiedrzik, C.M., Kohler, A., Singer, W., and Muckli, L. (2010). Stimulus predictability reduces responses in primary visual cortex. J. Neurosci. *30*, 2960–2966.

4. Delorme, A., and Makeig, S. (2004). EEGLAB: an open source toolbox for analysis of single-trial EEG dynamics including independent component analysis. J. Neurosci. Methods *134*, 9–21.

5. Kok, P., Jehee, J.F., and De Lange, F.P. (2012). Less is more: expectation sharpens representations in the primary visual cortex. Neuron *75*, 265–270.

6. Delorme, A. (2023). EEG is better left alone. Sci. Rep. *13*, 2372.

7. Lange, F.P. de, Heilbron, M., and Kok, P. (2018). How Do Expectations Shape Perception? Trends Cogn. Sci. *22*, 764–779. https://doi.org/10.1016/j.tics.2018.06.002.

8. den Ouden, C., Kashyap, M., Kikkawa, M., and Feuerriegel, D. (2025). Limited Evidence for Probabilistic Cueing Effects on Grating-Evoked Event-Related Potentials and Orientation Decoding Performance. Psychophysiology *62*, e70076. https://doi.org/10.1111/psyp.70076.

9. Schneider, F., and Blank, H. (2026). Sensory sharpening and semantic prediction errors unify competing models of predictive processing in human speech comprehension. PLoS Biol. *24*, e3003588.

10. Benjamini, Y., and Hochberg, Y. (1995). Controlling the False Discovery Rate: A Practical and Powerful Approach to Multiple Testing. J. R. Stat. Soc. Ser. B Stat. Methodol. *57*, 289–300. https://doi.org/10.1111/j.2517-6161.1995.tb02031.x.

11. Garlichs, A., and Blank, H. (2024). Prediction error processing and sharpening of expected information across the face-processing hierarchy. Nat. Commun. *15*, 3407.

12. Grootswagers, T., Wardle, S.G., and Carlson, T.A. (2017). Decoding dynamic brain patterns from evoked responses: a tutorial on multivariate pattern analysis applied to time series neuroimaging data. J. Cogn. Neurosci. *29*, 677–697.

13. Press, C., Kok, P., and Yon, D. (2020). The Perceptual Prediction Paradox. Trends Cogn. Sci. *24*, 13–24. https://doi.org/10.1016/j.tics.2019.11.003.

14. Maris, E., and Oostenveld, R. (2007). Nonparametric statistical testing of EEG-and MEG-data. J. Neurosci. Methods *164*, 177–190.

15. Westerberg, J.A., and Roelfsema, P.R. (2025). Hierarchical interactions between sensory cortices defy predictive coding. Trends Cogn. Sci. *0*. https://doi.org/10.1016/j.tics.2025.09.018.

16. Carlson, T., Tovar, D.A., Alink, A., and Kriegeskorte, N. (2013). Representational dynamics of object vision: the first 1000 ms. J. Vis. *13*, 1–1.

17. Cichy, R.M., Pantazis, D., and Oliva, A. (2014). Resolving human object recognition in space and time. Nat. Neurosci. *17*, 455–462.

18. Ahissar, M., and Hochstein, S. (2004). The reverse hierarchy theory of visual perceptual learning. Trends Cogn. Sci. *8*, 457–464. https://doi.org/10.1016/j.tics.2004.08.011.

19. McDermott, H.H., de Martino, F., Schwiedrzik, C.M., and Auksztulewicz, R. (2026). Dissociable dynamic effects of expectation during statistical learning. eLife *13*, RP103689. https://doi.org/10.7554/eLife.103689.

20. Gabhart, K.M., Xiong, Y. (Sophy), and Bastos, A.M. (2025). Predictive coding: a more cognitive process than we thought? Trends Cogn. Sci. *29*, 627–640. https://doi.org/10.1016/j.tics.2025.01.012.

21. Rungratsameetaweemana, N., Itthipuripat, S., Salazar, A., and Serences, J.T. (2018). Expectations Do Not Alter Early Sensory Processing during Perceptual Decision-Making. J. Neurosci. *38*, 5632–5648. https://doi.org/10.1523/JNEUROSCI.3638-17.2018.

22. Kutas, M., and Federmeier, K.D. (2011). Thirty Years and Counting: Finding Meaning in the N400 Component of the Event-Related Brain Potential (ERP). Annu. Rev. Psychol. *62*, 621–647. https://doi.org/10.1146/annurev.psych.093008.131123.

23. Rabovsky, M., Hansen, S.S., and McClelland, J.L. (2018). Modelling the N400 brain potential as change in a probabilistic representation of meaning. Nat. Hum. Behav. *2*, 693–705.

24. Lamme, V.A., and Roelfsema, P.R. (2000). The distinct modes of vision offered by feedforward and recurrent processing. Trends Neurosci. *23*, 571–579.

25. Xie, S., Singer, J., Yilmaz, B., Kaiser, D., and Cichy, R.M. (2025). Recurrence affects the geometry of visual representations across the ventral visual stream in the human brain. PLOS Biol. *23*, e3003354. https://doi.org/10.1371/journal.pbio.3003354.